53rd AIAA/ASME/ASCE/AHS/ASC Structures, Structural Dynamics and Materials Conference
20th AI
23 - 26 April 2012, Honolulu, Hawaii

AIAA 2012-1510

Span Morphing: A Conceptual Design Study

R M. Ajaj[1], M I. Friswell[2], E. I. Saavedra Flores[3], and O. Little[4]
College of Engineering, Swansea University,
Swansea, SA2 8PP UK

and

A T. Isikveren[5]
Bauhaus Luftfahrt e.V. Lyonel-Feininger-Str. 2880807
Munich, Germany

The use of variable wing span to enhance flight performance and control authority of high endurance, medium altitude UAV is investigated. Asymmetric span extension is used to replace ailerons and maintain roll control over the entire flight envelope of the vehicle. The span extension required to generate a rolling moment equal to that produced by ailerons is estimated at four flight points. The study is performed using Tornado Vortex Lattice Method (VLM). 36% increase in wing semi-span is required to maintain roll authority. On the other hand, symmetric span morphing is used to reduce induced drag and enhance the endurance capability of the vehicle. 20% symmetric span morphing was found to be the optimum to reduce the overall drag of the wing by 10% at the start of cruise and 2.5% at the end of cruise. The morphing wing structure is to be designed using Zero Poisson's ratio Accordion honeycomb with elastomeric skins. The geometry of the honeycomb will be optimised using the Genetic Algorithm (GA) optimiser to minimise the structural weight of the wing while meeting various design constraints.

I. Introduction

CONTINUOUS demands to enhance flight performance and control authority have focused the interest of aircraft designers on span morphing. Wings with large spans have good range and fuel efficiency, but lack manoeuvrability and have relatively low cruise speeds. By contrast, aircraft with low aspect ratio wings are faster and highly manoeuvrable, but show poor aerodynamic efficiency [1]. A variable span wing can potentially integrate into a single aircraft the advantages of both designs, making this emerging technology especially attractive for military UAVs. Increasing the wingspan, increases the aspect ratio and wing area, and decreases the spanwise lift distribution for the same lift. Thus, the drag of the wing decreases, and consequently, the range of the vehicle increases. Unfortunately, the wing-root bending moment can increase considerably due to longer span. Thus the aerodynamic, the structural, and the aeroelastic characteristics of the vehicle should be investigated in the design of variable-span morphing wings. Most span morphing concepts are based on a telescopic mechanism, following the ideas of Ivan Makhonine, a Russian expatriate where the wing outer panel telescoped inside the inner panel to enable span and wing area changes. The MAK-10 was the first design with telescopic wing and it first flew in 1931. The mechanism was powered pneumatically and enabled span increases up to 62% (from 13 to 21m) and area increases up to 57% (from 21 to 33m^2) [2]. Blondeau et al. [3] designed and fabricated a three segmented telescopic wing for a UAV. Hollow fiberglass shells were used to preserve the spanwise aerofoil geometry and ensure compact storage and deployment of the telescopic wing. To reduce the weight, they replaced the wing spars with inflatable actuators that could support the aerodynamic loads on the wing (in excess of 15 lbs/ft^2). Their telescopic spar design consisted of three concentric circular aluminium tubes of decreasing diameter and increasing length, connected by ceramic linear bearings, and deployed and retracted using input pressures of 50–70psi. The wing could undergo a 114% change in the aspect ratio, while supporting aerodynamic loads.

[1] Research Assistant, College of Engineering, Swansea University, Wales, UK, SA2 8PP, AIAA member.
[2] Professor of Aerospace Structures, College of Engineering, Swansea University, Wales, UK, SA2 8PP.
[3] Research Associate, College of Engineering, Swansea University, Wales, UK, SA2 8PP, AIAA member.
[4] MSc student, College of Engineering, Swansea University, Wales, UK, SA2 8PP.
[5] Head, Visionary Aircraft Concepts and Deputy Chief Technical Officer, Bauhaus Luftfahrt e.V. Lyonel-Feininger-Str. 28,80807 Munich, Germany, AIAA member.

Copyright © 2012 by the American Institute of Aeronautics and Astronautics, Inc. All rights reserved.

Blondeau et al [4] adopted two identical telescopic spars instead of one, mechanically coupled by the ribs, to prevent wing twist and fluttering. The new prototype could undergo a 230% change in aspect ratio, and seam heights were reduced giving less parasitic drag. In its fully deployed condition the telescopic wing could achieve lift-to-drag ratios as high as 16, which was similar to its solid foam-core wing counterpart. The most dramatic morphing wing involving span change that has been realized as a wind tunnel prototype is the Agile Hunter by Lockheed Martin [5-7]. Funded by DARPA within the MAS program, the prototype was based on a military UAV capable of folding the inner sections of the wing near to the fuselage, to reduce the surface area and drag during transonic flight at low altitude (also called a Z-wing). The major challenge was the realization of suitable hinges that connect the two wing portions; the hinges have to sustain the aerodynamic loads but offer a smooth, continuous aerodynamic surface. Several material were considered, including silicone-based and Shape Memory Polymer skins. Wind tunnel tests at Mach 0.6, showed a morphing capability from 0° to 130° over 65s with a controllable, reliable and precise actuation.

Asymmetrical span morphing can be used for roll control. Henry and Pines [8] extended the standard aircraft dynamics model to include the additional terms (as perturbations) due to morphing and demonstrated that asymmetrical span morphing was effective for roll control. The total damping in the system increased when the span extension rate was positive (span increase) due to the conservation of angular momentum. Span extension induces a roll damping moment that is greater than that due to aileron deflection. Seigler et al. [9] also investigated asymmetrical span extension for increased manoeuvrability of bank-to-turn cruise missiles. By formulating a full nonlinear model of the missile, due to the shift of the missile's centre of mass and the dependence of the rolling moment on the angle of attack, they showed that the control authority can be significantly larger when compared to conventional tail surface control. Improved manoeuvrability, however, is highly dependent on the angle of attack, linear actuation speed, and extension length. Moreover, as the mass of the extending wings becomes large relative to the missile body, the rigid body dynamics can become increasingly complex and a nonlinear control law was formulated to control the roll, angle of attack, and side slip angle dynamics in accordance with bank-to-turn guidance. The control method proved to be adept in tracking commanded inputs while effectively eliminating sideslip.

II. Aerodynamics

The Tornado Vortex Lattice Method (TVLM) was used for aerodynamic predictions. Tornado is a linear aerodynamics code, and thus it discounts wing thickness and viscous effects [10]. These limitations imply that Tornado can only be used for angles of attack up to 8-10° for slender wings. Linear aerodynamic theory is still nevertheless very useful as most aircraft typically operate within the linear region (operating lift coefficients at reference speeds) in cruise, as well as both take-off and landing phases. These are the flight stages in which most of this research and analysis has been undertaken. In Tornado one half of the wing is built and then mirrored with respect to the centerline of the aircraft to generate the entire wing. In order to investigate roll control using span morphing, each half of the wing is built separately to allow the asymmetric change in span. Typically the wing is defined from the root to the tip in Tornado for the symmetric case. However for the asymmetric case, one half of the wing is defined from root to tip and the other half is defined from tip to root. As the wing semi-span starts to increase the size of the spanwise elements start to increase resulting in coarser aerodynamic mesh. A convergence study was performed to determine the size of the aerodynamic mesh required to generate accurate and robust results. The number of elements in the chord wise direction was fixed to 5 elements and only the spanwise density was changed. The variation with the overall forces in the x and z directions with the number of spanwise elements are shown in Fig. 1 and Fig. 2.

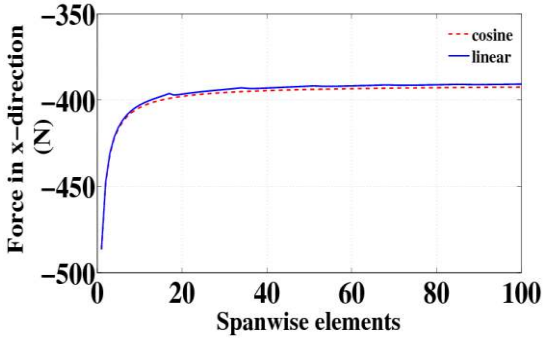

Figure 1. Force in the x-direction for different spanwise elements.

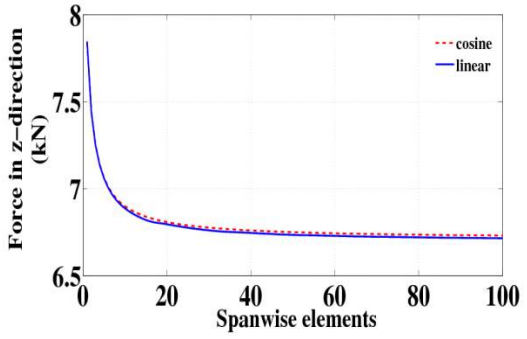

Figure 2. Force in the z-direction for different spanwise elements.

As the numbers of elements increase, the accuracy of the prediction improves but the computation time increases greatly. It points out that 20 elements are sufficient to provide robust prediction with a relative error of 0.05%. A cosine distribution for the spanwise and chordwise panels was adopted.

III. Asymmetric span extension

The BAE Systems Herti UAV shown in Fig. 3 and 4 was selected for this study. The UAV has a maximum lift to drag ratio of about 20 and a maximum endurance capability of 18 hours. A representative flight profile was assumed in this paper. The weight fractions of the vehicle along for each flight segment are listed in Table 1. The Herti take-off with a maximum weight of 800kg and it cruises for 18 hours with a speed of 50m/s at 6100m (10,000ft) and then it descends and lands.

Figure 3. The BAE Systems Herti UAV.

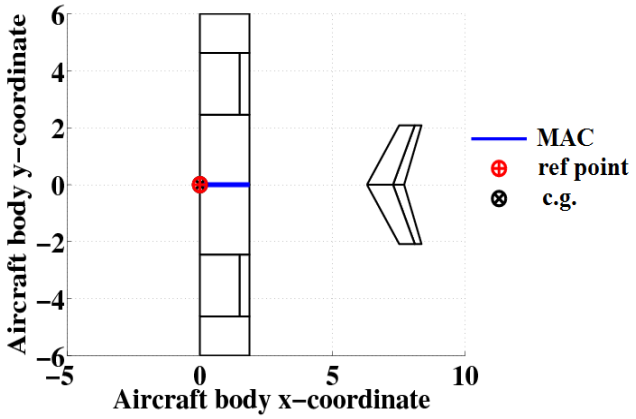

Figure 4. The Herti UAV in Tornado VLM.

Four points on the flight envelope were considered. These correspond to take-off, start of cruise, end of cruise, and landing. The instantaneous flight conditions and vehicular weight at those points are given in Table 2. In order to obtain the weight of the vehicle at each of the flight points the weight fractions listed in Table1 are employed. Furthermore, Table 2 contains the maximum allowable aileron angle at each of these flight points. These values are assumed based on similar UAVs due to the lack of data. In this paper, the shift of the centre of gravity associated with span morphing is neglected.

Table 1. Weight fractions of the UAV.

Mission segment	Weight fraction
Take-off-climb	0.9875
Cruise	0.78
Descent	0.9875

Table 2. Flight conditions at the selected flight points.

Flight point	MTOW (kg)	Speed (m/s)	Altitude (m)	Angle of attack (deg)	Aileron angle (deg)
Take-off	800	25	0	11	20
Start of cruise	790	50	6100	5	10
End of cruise	608	50	6100	3.83	10
Landing	600	20	0	12.8	20

At each of the flight points listed in Table 2, the maximum rolling moment generated by the ailerons and the adverse yawing moment associated with it are computed. The ailerons are assumed to deflect asymmetrically with the same angle. For span morphing, the span of one side of the wing is increased gradually until it reaches a point where the rolling moment from span morphing is equal to the rolling moment generated by the ailerons. The required span extensions at take-off, start of endurance, end of endurance, and landing are computed and listed in Table 3.

Table 3. Moments generated by span morphing.

Flight point	Semi-Span extension (%)	Rolling moment (Nm)	Yawing moment from span (Nm)	Yawing moment from aileron (Nm)
Take-off	27.1	6735	1150	1350
Start of cruise	29	7275	623	1200
End of cruise	36.4	7300	495	1150
Landing	23.4	4260	850	900

It turns out that the maximum span morphing required is at the end of cruise, where 36% extension in the wing semi-span is required. Figure 5, 6, 7, and 8 show the variation of the rolling moment coefficient and the yawing moment coefficient with span extension and aileron angle at the end of cruise flight point.

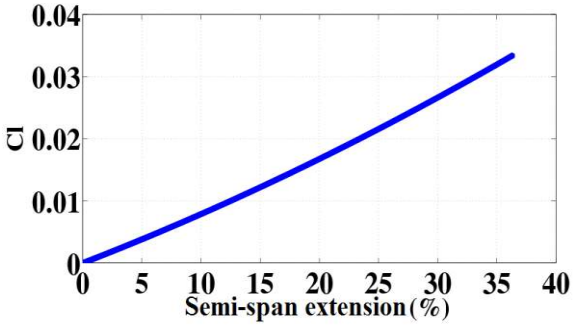

Figure 5. Variation of rolling moment coefficent with span extension at the end of cruise.

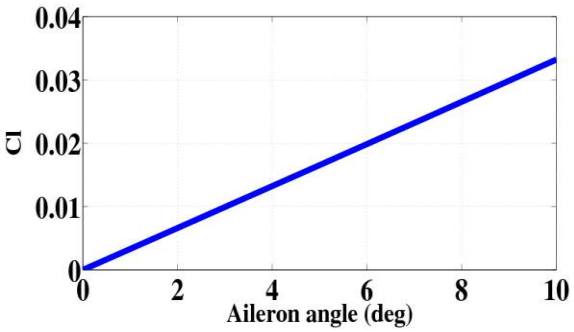

Figure 6. Variation of rolling moment coefficent with aileron angle at the end of cruise.

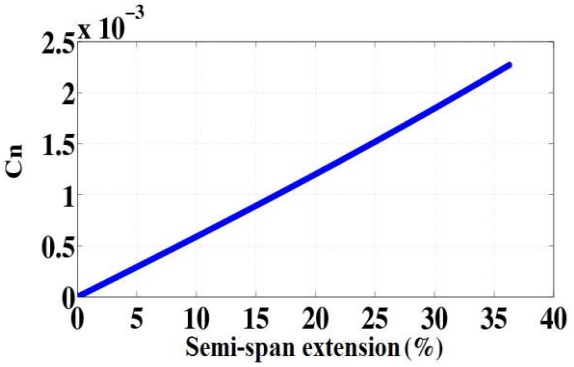

Figure 7. Variation of rolling moment coefficent with span extension at the end of cruise

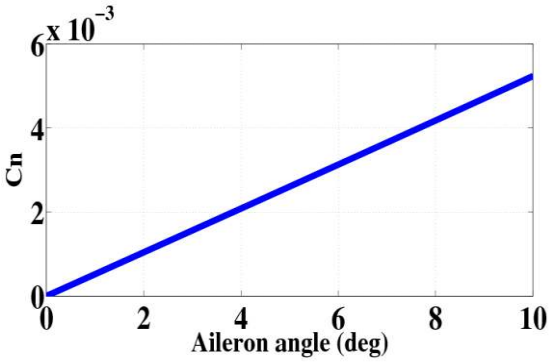

Figure 8. Variation of rolling moment coefficent with span extension at the end of cruise.

It can be seen that the variation of the rolling moment coefficient and the yawing moment coefficient is linear with the aileron angle. This is because Tornado is a linear aerodynamic code. On the other hand, the rolling moment coefficient and the yawing moment coefficient variations with span extension seem to be parabolic. The rate of change with span extension tends to increase as the percentage of span extension increases.

A. Sensitivity to span loading

It is of great interest to understand the variation of the span extension required as the UAV burns its fuel while cruising at a constant altitude. As one side of the wing extends, the change in lift becomes

$$\Delta \mathrm{L} = qC_L c b_s \tag{1}$$

where q is the dynamic pressure, C_L is the lift coefficient, c is the chord of the rectangular wing, b_s is change in wing semi-span as shown in Fig. 9.

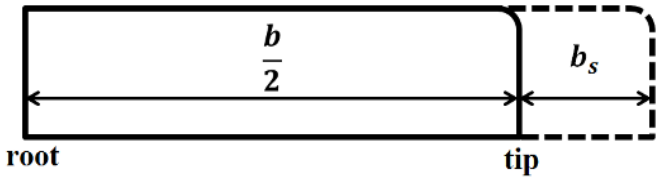

Figure 9. The geometry of the morphed semi-span of the wing.

The rolling moment due span extension becomes

$$L_s = \Delta \mathrm{L}\left(\frac{b}{2} + \frac{b_s}{2}\right) = qC_L c\left(\frac{b_s b + b_s^2}{2}\right) \tag{2}$$

where b is the original wing span. The above correlation s assumes that the differential lift due to span morphing acts at the half span point of the morphing partition. Furthermore, it can be noted that the rolling moment generated by the span morphing has a parabolic variation with the span extension as discussed above. For steady flight, the lift coefficient can be estimated as

$$C_L = \frac{W}{qS} = \frac{W}{qcb} \tag{3}$$

where W is the instantaneous weight of the UAV and S is the original wing reference area. The differential lift force becomes

$$\Delta \mathrm{L} = \frac{W}{b} b_s \tag{4}$$

The rolling moment due to span extension must be greater than or equal to that generated by the ailerons

$$L_s = \Delta \mathrm{L}\left(\frac{b}{2} + \frac{b_s}{2}\right) \geq L_a \tag{5}$$

where L_a is the rolling moment generated by the ailerons. The minimum span extension required to meet the rolling moment of the ailerons becomes

$$b_s \geq -\frac{b}{2} + \sqrt{\left(\frac{b}{2}\right)^2 + 2\frac{L_a}{\left(\frac{W}{b}\right)}} \tag{6}$$

Equation 6 indicates that the minimum span extension required depends on the span loading of the aircraft during steady flight. As fuels are burned, larger span extensions are required to meet the rolling authority of conventional ailerons. This is illustrated in Fig. 10.

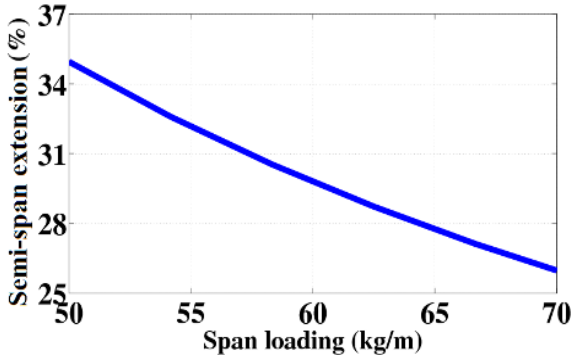

Figure 10. Variation of required span extension with span loading.

The maximum rolling moment generated by the ailerons of the Herti UAV is 7300 Nm at 50 m/s. The span extension required for different span loading to generate the same rolling moment can be determined using

Equation 6. Figure 10 shows that as the UAV starts burning fuel at constant altitude and its span loading reduces the span extension required to generate 7300 Nm increases from 26% to 35%. The sensitivity of the span morphing to span loading infer that it is also sensitive to the instantaneous angle of attack because they directly related.

B. Sensitivity to angle of attack

The angle of attack at the end of cruise flight point is varied and the variation in span morphing is computed and compared to conventional ailerons. It turns out, that the rolling moment and yawing moment coefficients for a given span extension increase significantly as the angle of attack is increased. In contrast, the rolling moment and yawing coefficients of the ailerons are independent of the angle of attack for a given aileron angle. This because the rolling and adverse yawing moments generated by the ailerons depend only on the aileron angle, aileron dimensions, aileron spanwise position, and the dynamic pressure but not the angle of attack. This is shown in Fig. 11, 12, 13, and 14.

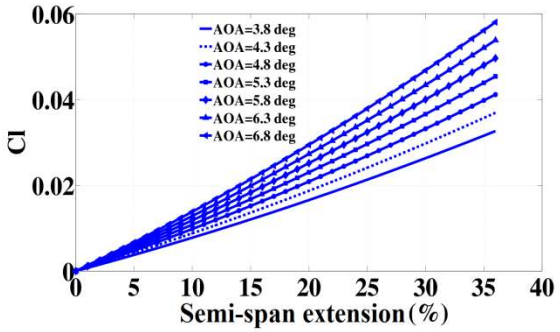

Figure 11. Variation rolling moment coefficient with span extension for different angles of attack.

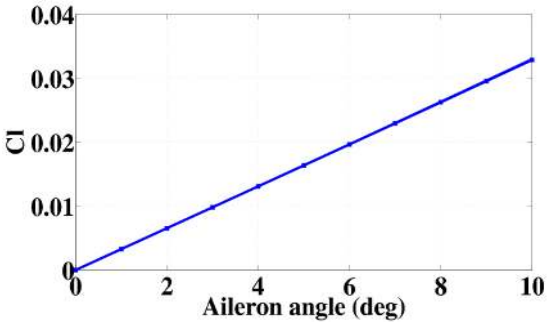

Figure 12. Variation rolling moment coefficient with aileron angle for different angles of attack.

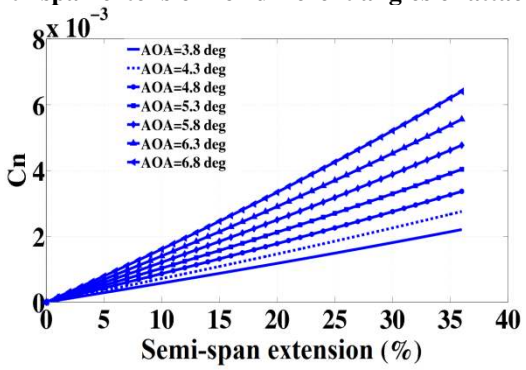

Figure 13. Variation yawing moment coefficient with span extension for different angles of attack.

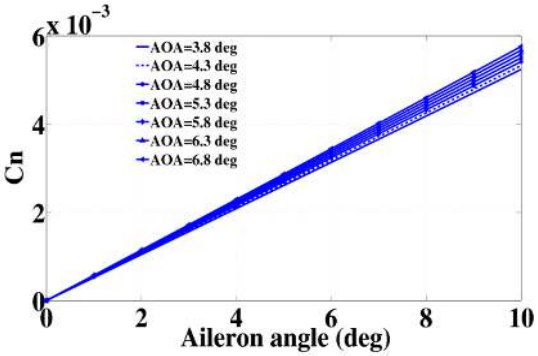

Figure 14. Variation yawing moment coefficient with aileron angle for different angles of attack.

The above figures show that it is very efficient to pitch and extends the wing span simultaneously to maximise the rolling authority of the vehicle. Such a manoeuvre (pitch and roll) can be of great interest for military UAVs that require large rolling authority, but this depends on the type of manoeuvre to be performed. These results raise an important issue about morphing technologies. The issue is

- Shall morphing technologies be operated in the same way conventional technologies are operated?
- Does operating morphing structures in the same way conventional structures are operated limit the benefits of morphing and reduce its effectiveness in competing with conventional structures which have been used and optimised for almost a century?

C. Optimum rolling strategies

In the above section, roll manoeuvre was achieved by extending the span on one side of the wing while keeping the span on the other side constant. Obviously from a structural perspective, this is not the best strategy to achieve roll control because it increases the root bending moment significantly and it requires larger local strains if complaint structures are to be employed. This sections aims to use a search method to obtain the optimum strategy to morph the span to meet the roll demand. The objective is to minimise the drag coefficient while rolling the vehicle. Constraints on the rolling moment required and root bending moment are added. The optimisation problem is summarised in Table 4.

Table 4. Optimising rolling manoeuvre.

Objective function	minimise (C_D)
Variables	δ_1 change in starboard wing span (%) δ_2 change in port wing span (%)
Constraints	$0 \leq \delta_1 \leq 36\%$ $-36\% \leq \delta_2 \leq 0$ $RM_s \geq RM_a$

where C_D is the overall drag coefficient of the UAV, b_1 is the span of the starboard wing, b_2 is the span of the port wing, BM_s is the maximum root bending moment due to span morphing, and BM_a is the maximum root bending moment due to ailerons deflection. In order to compute the drag coefficient associated with pure roll, the rudder is deflected to counteract the adverse yawing moment generated by asymmetric span morphing. This contributes to the induced drag coefficient. The search method used for this problem is the Genetic Algorithm (GA) optimiser. Genetic Algorithm is stochastic global search and optimisation methods. GA mimics the metaphor of natural evolution by applying the principle of the survival of the fittest to produce successively better approximations to a solution. The "Matlab GA Toolbox", developed by Chipperfield et al. [11], was incorporated in this analysis. A fitness value is assigned to every individual of the initial population through an objective function that assesses the performance of the individual in the problem domain. Then, individuals are selected based on their fitness index and crossover between them is performed to generate new offspring. Finally, mutation of the new offspring is performed to ensure that the probability of searching any subspace of the problem is never zero. These abovementioned processes iterate until the optimum solution is achieved depending on the convergence criteria of the problem.

In the above section approximately 36% semi-span extension was required to meet the roll control requirements of the vehicle. The overall drag coefficient associated with it is 0.0194 and the root bending is 16.60 kNm. The drag coefficient associated with the ailerons is 0.0198 and the root bending moment is 10.7 kNm. Two rolling cases are investigated in this section. The first case is when the vehicle rolls without losing altitude and the root bending moment must not be greater than that of the ailerons by more than 30%. For the vehicle to roll without losing altitude, the new overall span of the wing (after morphing) must be always greater than or equal to the original span (before morphing) to ensure that the vehicle rolls at a steady altitude. In contrast, in the second case the altitude constraint is removed and a root bending moment constraint is added where the root bending moment must not be greater than that of the ailerons by more than 10%. Table 5 summarise the results for each rolling case.

Table 5. Optimum rolling strategies.

Rolling case	Drag coefficient (C_D)	Bending moment (kNm)	Constraint	Change in span of starboard wing (%)	Change in span of port wing (%)
Ailerons	0.0198	10.7	-	-	-
One side	0.0194	16.6	-	36	-
Both sides, constant altitude	0.0196	13.15	$\delta_1 + \delta_2 \geq 0\%$ $BM_s \leq 1.3BM_a$	23	- 23
Both sides, bending moment	0.0196	11.5	$BM_s \leq 1.1BM_a$	16.7	- 36

Table 5 shows that from an aerodynamic point of view it is superior to achieve roll manoeuvre by extending one side of the wing by 36% while keeping the other side fixed to maximise the overall span of the wing. However, from a structural point of view, this results in very large root bending moment 60% higher than that produced by the ailerons. To roll at the same altitude, it is optimum to morph both sides of the wing by the same amount but opposite directions this increases the drag coefficient slightly by 1% but drops the root bending moment by of 21% in comparison to morphing one side only. On the other hand, when a stringent root bending moment constraint is added and the constant altitude constraint is removed, the drag coefficient increases by 1% and the root bending moment is reduced by 31% in comparison to morphing one side only. The different morphing strategies are shown in Fig. 15.

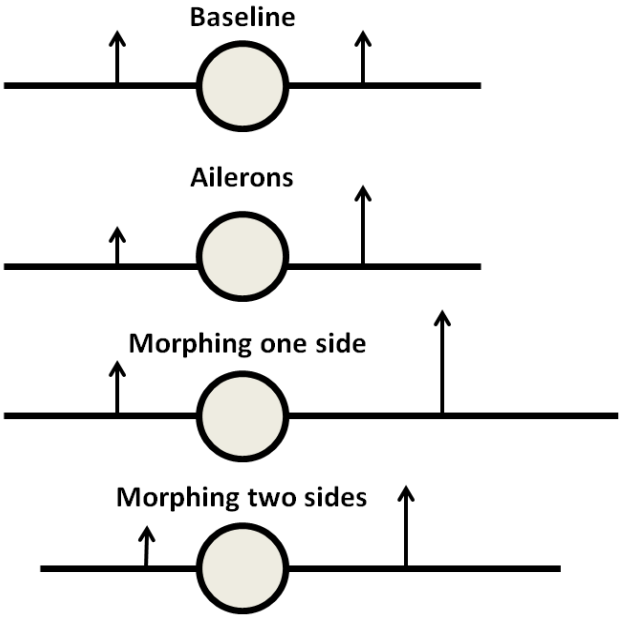

Figure 15. Schematic of the different rolling strategies.

Table 5 illustrates that all the morphing strategies are superior to conventional ailerons in generating lower overall drag which gives the vehicles more manoeuvrability and agility. However, conventional ailerons produce smaller root bending moment than span morphing which can impact the weight of the wing unless novel materials and mechanisms are adopted. Nevertheless, span morphing reduces the radar cross-section (RCS) of the vehicles and enhances its stealth characteristics.

IV. Flight performance

In the previous section, the feasibility of span morphing for roll control was discussed. To maximise synergy, the span morphing used asymmetrically for roll control of the UAV can be used symmetrically to enhance flight performance and its endurance capability. The total drag of the wing consists of two major components, parasitic drag (zero lift drag) and induced drag. The total drag of the wing (D) becomes

$$D = D_o + D_i \tag{7}$$

where D_o is the parasitic drag and D_i is the induced drag. The induced drag can be expressed as

$$D_i = qSC_{D_i} = qbc\frac{C_L^2}{\pi eAR} \tag{8}$$

where e is the Oswald efficiency and AR is the wing aspect ratio. For a steady level flight, the lift coefficient from Equation 3 can be substituted in the induced drag equation as

$$D_i = \frac{1}{\pi qe}\left(\frac{W}{b}\right)^2 \tag{9}$$

The parasitic drag can be expressed as

$$D_o = qSC_{D_o} = qcb\frac{C_{f_e}S_{wet}}{S} \tag{10}$$

From Tornado VLM, the equivalent skin friction coefficient of the wing can be approximated as 0.00323 and the ratio of the wetted area to the reference area $\left(\frac{S_{wet}}{S}\right)$ is fixed and equal to 2.05. Similar values are quoted by Raymer [12].

$$D = q\frac{C_{f_e}S_{wet}}{S}cb + \frac{1}{\pi qe}\left(\frac{W}{b}\right)^2 \tag{11}$$

At any steady flight point, the parasitic drag increases linearly as the span of the wing increases. In contrast, the induced drag drops with the square of the span. The previous statement is valid if the change in Oswald's efficiency is ignored. The variation in total wing drag with wing span at the start of cruise and end of cruise are shown in Fig. 16 and 17.

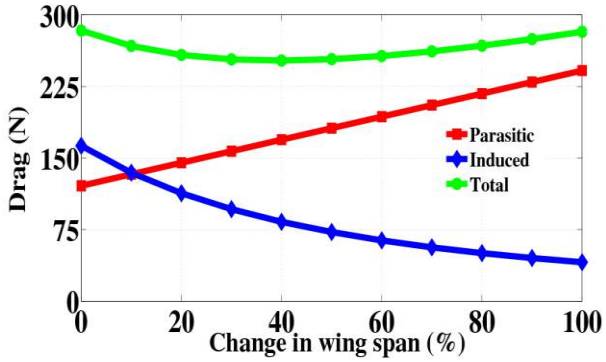

Figure 16. Varitiation of drag with wing span at the start of cruise.

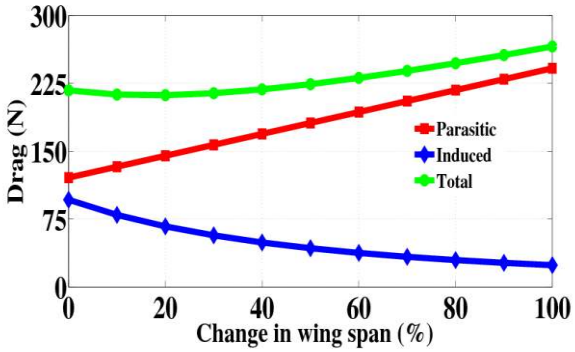

Figure 17. Varitiation of drag with wing span at the end of cruise.

For the start of cruise, initially the induced drag of the wing is higher than the parasitic drag. As the wing span increases (symmetrically), the induced drag drops while the parasitic drag increase. They become equal at 10% symmetric increase in wing span. The minimum total drag of the wing occurs at 40% increase in wing span resulting in 11% reduction in the total wing drag. It turns out that in the region between 20% to 60% increase in wing span, the total drag is almost uniform. At 20%, the total drag reduces by 10%, while at 60% the total drag reduces by 9.5%. From a structural point of view, it's more feasible to increase the wing span by 20% to reduce the total drag by 10% rather than increasing the span by 40% to get 11% reduction in the total drag. For the end of cruise flight point, initially the parasitic drag is higher than the induced drag. This because the UAV is flying at the same altitude as the start of cruise but now it has to generate smaller lift and hence lower induced drag. It turns out that increasing the minimum total wing drag occurs at 17% increase in wing span result in 2.5% reduction in the wing drag. Any further increase in the span further increases the total drags as the increase in parasitic dominates the reduction in induced drag. This is summarised in Table 6.

Table 6. Drag reduction from symmetric span morphing.

Flight point	MTOW (kg)	Speed (m/s)	Altitude (m)	Drag reduction (%)	Optimum span increase (%)
Start of cruise	790	50	6100	11	40
End of cruise	608	50	6100	2.5	17

The effectiveness of symmetric span morphing to reduce the drag depends on the drag breakdown. In other words, it depends on the relative magnitude of the parasitic drag and the induced drag. For flight points where the wing is generating large amount of lift, morphing the span can be very effective, but when the wing is generating little lift, span morphing increase the drag rather than reduce it. Nevertheless, increasing the wing span for low lift flight phases can be effective such as landing where the increase in drag is required to reduce the landing distance. By examining Equation 11, for any given flight conditions and instantaneous vehicular weight, the span that minimise the total wing drag can be obtained by taking the derivative of the total drag with respect to the wing span as

$$\frac{\partial D}{\partial b} = qC_{f_e}\frac{S_{wet}}{S} - \frac{2W^2}{\pi q e b^3} = 0 \tag{12}$$

hence the span that produce the minimum wing drag becomes

$$b_{min} = \left(\frac{2W^2 S}{\pi q^2 e\, C_{f_e} S_{wet}}\right)^{\frac{1}{3}} \tag{13}$$

For a given flight conditions, the wing span that produces the minimum drag is proportional to $\left(W^{2/3}\right)$. This means that as the vehicle burns fuel and its weight reduces, the span that produces the minimum drag reduces.

V. Future work: Morphing structure design

As discussed in the introductory section, different solutions and design concepts have been investigated to allow span morphing. The feasibility of any concept is highly dependent on the scale and objectives of the vehicle. For instance, honeycomb cores with elastomeric skins cannot be employed as the primary structure on large scale vehicles (such as Airbus A330) to allow change in the span due to the high aerodynamic loads. Telescopic structures seem to be a superior solution for large scale vehicles. Nevertheless, the use of honeycomb cores with flexible skins can be a superior, lighter, and simpler solution for small scale vehicles. Based on the asymmetric and symmetric span morphing analyses performed above, it turns out that 25% change in wing span is the optimum value from a structural and aerodynamic point of view to maintain roll control and enhance flight performance. Therefore, the design of a morphing structure in this section aims at 25% change in wing span (extension and contraction). Conventional hexagonal and auxetic honeycombs are not feasible for span morphing because their non-zero Poisson's ratio creates a coupling effect between the span and the chord of the morphing wing. This can jeopardise the the benefits of span morphing and limit its effectiveness. One possible solution to eliminate the coupling, is by constraining the chord from expanding (for auxetic) or contracting (for hexagonal), however this results in significant increase in the effective stiffness in the morphing direction (span) resulting in large increase in the actuation force(s). To overcome this problem, the zero Poisson's ratio accordion honeycomb, shown in Fig. 18, is adopted in this study.

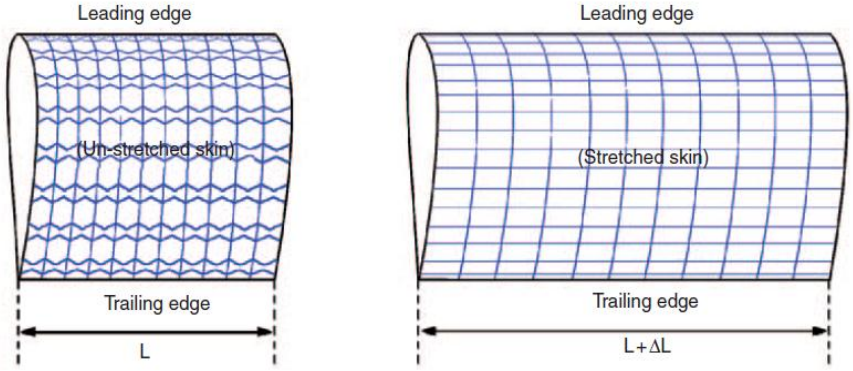

Figure 18. Accordion cellular honeycomb in one-dimensional morphing [13].

Due to it geometry (Fig. 19), the accordion honeycomb when extended or compressed along its x-direction, deforms without any net deformation in the y-direction. Olympio and Gandhi [13] developed analytical expressions to estimate the mechanical properties of the accordion honeycomb. They adopted an approach similar to that used by Gibson and Ashby [14]. By examining the geometry of the accordion honeycomb cell, it points out that the upper part consists of a hexagonal cell with positive wall angle while the lower part consists of a hexagonal cell with negative wall angle.

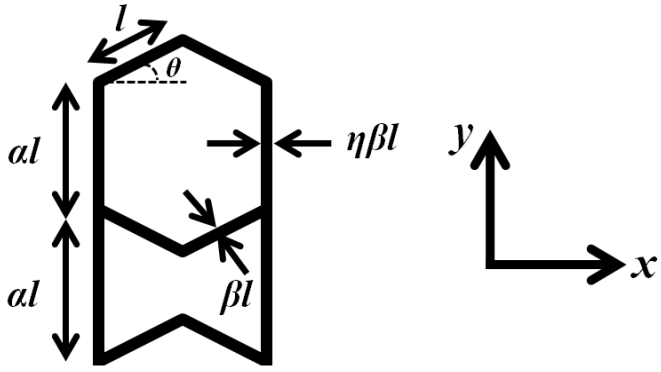

Figure 19. Unit cell with its geometric parameters.

According to Olympio and Gandhi [13], the Young's modulus in the x-direction can be expressed as

$$E_x = \frac{\beta^3}{\alpha cos\theta(\beta^2 + (1 + \kappa\beta^2)tan^2\theta)} E_s \tag{14}$$

where β is the ratio of the thickness to the length of the inclined cell wall, θ is the cell angle, α is the ratio of the of the length of the vertical cell wall to the length of the inclined cell wall, and κ is equal to 2.4+1.5v, where v is the Poisson's ratio of the material of the honeycomb, and E_s is the Young's modulus of the material of the honeycomb. From the geometry of the cell, the density of the honeycomb can be expressed as

$$\rho = \frac{\beta(2+\eta\alpha)}{2\alpha cos\theta}\rho_s \tag{15}$$

where η is the ratio of the thickness of the vertical wall to the thickness of the inclined wall of the cell and ρ_s is the density of the material of the honeycomb. By examining Equations 14 and 15, it can be noticed that the axial Young's modulus and effective density of the honeycomb depends on the ratios of thickness and length and not on the absolute values. This indicates that for targeted honeycomb axial properties, a variety of honeycomb geometries are feasible. Therefore, it becomes non-trivial to select the optimum honeycomb configuration without a search method.

The GA toolbox discussed above will be employed to minimise the structural weight of the honeycomb and minimise the axial stiffness of the honeycomb while meeting the various design constraints. Preliminary studies will assess the feasibility of using the honeycomb structure over the entire wing at ultimate aerodynamic loads.

VI. Conclusion

Variable wing span is an effective device to enhance flight performance and replace conventional control surfaces. For roll control, 36% asymmetric increase in the wing semi-span is required to replace the ailerons and maintain roll control over the entire envelope of high endurance medium altitude UAV. For flight performance, 20% symmetric increase in the wing span was found to be optimum from structural and aerodynamic points of view. 20% symmetric increase in span reduced the drag of the wing by 10% at the start of cruise and by 2.5% at the end of cruise. The use of accordion honeycomb structure to allow span morphing will be investigated in future work.

Acknowledgments

The authors acknowledge funding from the European Research Council through Grant Number 247045 entitled "Optimisation of Multiscale Structures with Applications to Morphing Aircraft".

References

[1]McCormik, B.W. 1995. Aerodynamics, Aeronautics and Flight Mechanics, 2nd Edition, Wiley, New York.

[2]Weisshaar, T.A. 2006. "Morphing Aircraft Technology – New Shapes for Aircraft Design," RTO-MP-AVT-141, Neuilly-sur-Seine, France.

[3]Blondeau J. and Pines D. 2007. "Design and Testing of a Pneumatic Telescopic wing for Unmanned Aerial Vehicles," Journal of Aircraft, 44(4).

[4]Blondeau J., Richeson, J. and Pines D.J. 2003. "Design, Development and Testing of a Morphing Aspect Ratio Wing Using an Inflatable Telescopic Spar," 44th AIAA/ASME/ASCE/AHS/ASC Structures, Structural Dynamics and Materials Conference, Norfolk, VA, AIAA 2003-1718.

[5]Ivanco, T.G., Scott, R.C., Love, M.H., Zink, S. and Weisshaar, T.A. 2007, "Validation of the Lockheed Martin Morphing Concept with Wind Tunnel Testing," 48th AIAA/ASME/ASCE/AHS/ASC Structures, Structural Dynamics, and Materials Conference, Honolulu, Hawaii, AIAA 2007-2235.

[6]Bye, D.R. and McClure, P.D. 2007. ''Design of a Morphing Vehicle,'' 48th AIAA/ASME/ASCE/AHS/ASC Structures, Structural Dynamics, and Materials Conference, 23-26 April, Honolulu, HI, AIAA 2007-1728 (16 pp).

[7]Love, M.H., Zink, P.S., Stroud, R.L., Bye, D.R., Rizk, S. and White, D. 2007. "Demonstration of Morphing Technology through Ground and Wind Tunnel Tests," 48th AIAA/ASME/ASCE/AHS/ASC Structures, Structural Dynamics, and Materials Conference, Honolulu, Hawaii, AIAA 2007-1729.

[8]Henry, J.J. and Pines, D.J. 2007. ''A Mathematical Model for Roll Dynamics by Use of a Morphing-Span Wing,'' 48th AIAA/ASME/ASCE/AHS/ASC Structures, Structural Dynamics, and Materials Conference, 23-26 April, Honolulu.

[9]Seigler, T.M., Bae, J.S. and Inman, D.J. 2004. ''Flight Control of a Variable Span Cruise Missile,'' In: Proceedings of 2004 ASME International Mechanical Engineering Congress and Exposition, 13-19 November, Anaheim, CA, Paper No. IMECE2004-61961.

[10]Melin, T. A Vortex Lattice MATLAB Implementation for Linear Aerodynamic Wing Applications. Master's Thesis, Royal Institute of Technology (KTH), Department of Aeronautics, Sweden, 2000.

[11]Chipperfield, A. J. and Fleming, P. J., "The Matlab Genetic Algorithm Toolbox," IEE Colloquium on Applied Control Techniques using Matlab, Digest No.1995/014, January, 1996.

[12]Raymer, D.P. *Aircraft Design: A Conceptual Approach*, 4th Edition, AIAA, 2006.

[13]Olympio, K.R. and Gandhi, F. "Zero Poisson's Ratio Cellular Honeycombs for Flex Skins Undergoing One-Dimensional Morphing," Journal of Intelligent Material Systems and Structures, Vol.21, 2010.
[14]Gibson, L.J. and Ashby, M.F. *Cellular Solids-Structure and Properties,* 2nd Edition, Cambridge University Press, 1997.